Journal of Physics: Photonics

PAPER

Non-destructive three-dimensional imaging of artificially degraded CdS paints by pump-probe microscopy

Yue Zhou[1], David Grass[1], Warren S Warren[1,2,3,4] and Martin C Fischer[1,2,*]

[1] Department of Chemistry, Duke University, Durham, NC, United States of America
[2] Department of Physics, Duke University, Durham, NC, United States of America
[3] Department of Biomedical Engineering, Duke University, Durham, NC, United States of America
[4] Department of Radiology, Duke University, Durham, NC, United States of America
[*] Author to whom any correspondence should be addressed.

E-mail: martin.fischer@duke.edu

OPEN ACCESS

RECEIVED
27 October 2023

REVISED
21 March 2024

ACCEPTED FOR PUBLICATION
14 April 2024

PUBLISHED
26 April 2024

Original content from this work may be used under the terms of the Creative Commons Attribution 4.0 licence.

Any further distribution of this work must maintain attribution to the author(s) and the title of the work, journal citation and DOI.

Keywords: cadmium sulfide, pigment degradation, pump-probe microscopy, cultural heritage, three-dimensional imaging

Supplementary material for this article is available online

Abstract

Cadmium sulfide (CdS) pigments have degraded in several well-known artworks, but the influence of pigment properties and environmental conditions on the degradation process have yet to be fully understood. Traditional non-destructive analysis techniques primarily focus on macroscopic degradation, whereas microscopic information is typically obtained with invasive techniques that require sample removal. Here, we demonstrate the use of pump-probe microscopy to nondestructively visualize the three-dimensional structure and degradation progress of CdS pigments in oil paints. CdS pigments, reproduced following historical synthesis methods, were reproduced as oil paints and artificially aged by exposure to high relative humidity and light. The degradation of CdS to $CdSO_4 \cdot xH_2O$ was confirmed by both FTIR (Fourier-transform infrared) and XPS (x-ray photoelectron spectroscopy) experiments. During the degradation process, optical pump-probe microscopy was applied to track the degradation progress in single grains, and volumetric imaging revealed early CdS degradation of small particles and on the surface of large particles. This indicates that the particle dimension influences the extent and evolution of degradation of historical CdS. In addition, the pump-probe signal decrease in degraded CdS is observable before visible changes to the eye, demonstrating that pump-probe microscopy is a promising tool to detect early-stage degradation in artworks.

1. Introduction

Cadmium sulfide (CdS)-based yellow pigments, also known as cadmium yellow, are a group of important inorganic pigments in art history [1]. The introduction of these pigments to artists' palettes was followed by the improvement of industrial manufacturing in the 19th–20th century [2]. These pigments were favored by prominent artists, including Claude Monet [3], Vincent van Gogh [4], Edvard Munch [5], Henri Matisse [6–9], and Pablo Picasso [10], due to their vivid colors and bright hues. However, many masterpieces by these artists have been found to suffer from CdS degradation such as fading, darkening, chalking, and flaking. The quality of historical CdS [10], the presence of synthetic residues [5], additives used by artists [4, 11], and environmental preservation conditions [12] can influence the degradation behaviors, complicating the conservation of artworks.

Great efforts have been made by art conservators and researchers to understand the mechanisms underlying the deterioration. CdS is a semiconductor with a direct bandgap of 2.42 eV (512 nm) (energy diagram shown in figure SI2) [13]. Within the bandgap, deep trap states originate from CdS defects, such as surface sulfur and cadmium vacancies [14, 15]. These trap states are suspected to drive CdS degradation, as reported in a recent study of Pablo Picasso's *Femme* [10]. This effect was speculated to be more pronounced for small CdS pigments due to the increased surface-to-volume ratio [10]. In addition, photocatalytic

© 2024 The Author(s). Published by IOP Publishing Ltd

activities of CdS nanoparticles with surrounding organic binders were suggested to be enhanced by an elevated number of defects, but further evidence is needed to fully understand the role of CdS particle size in the overall degradation process [10].

The synthesis method can affect the quality of Cd-based pigments and the stability of paints. Historical CdS pigments were mainly produced by either a dry or a wet method [1]. The dry method involved the calcination of metallic cadmium, cadmium oxide, or cadmium carbonate with a stoichiometric amount or an excess of sulfur at 300 °C–500 °C; the resulting CdS was washed and ground prior to applications in paintings. The wet process precipitated CdS from sulfide (hydrogen sulfide, sodium sulfide, or barium sulfide) and cadmium salt (cadmium chloride, cadmium nitrate, or cadmium sulfate) solutions; the precipitate was then washed and used without further thermal treatment. The pigments produced by wet methods are more prone to degradation due to their poor crystalline structures, smaller dimensions, and the presence of synthetic residues and/or byproducts from insufficient washing procedures [14, 15]. For example, cadmium chloride ($CdCl_2$) was detected in some extensively deteriorated sections in historical paintings [6–8, 11]. However, the exact role of residues remains unclear, and additional studies are required to reveal their influences on CdS degradation.

Environmental conditions strongly affect the degradation of CdS paints. In artificial aging experiments, humidity was identified to be the primary cause of CdS degradation, while light and elevated temperatures could exacerbate degradation [12], consistent with the hypothesis that soluble impurities affect degradation mechanisms [5].

Traditional nondestructive techniques such as Raman, UV-VIS-NIR reflectance, x-ray fluorescence, and photoluminescence spectroscopy have been employed to study CdS degradation [16, 17]. However, due to their limitation in resolution, these techniques typically acquire only macroscale information. Synchrotron radiation-based x-ray spectro-microscopic methods [5, 12] do provide high chemical and spatial resolution but are mostly restricted to analyzing cross-sectional samples.

Here, we demonstrate the use of pump-probe microscopy, a nonlinear optical technique, to nondestructively generate three-dimensional, high-resolution maps of paint structures and to track the degradation process on a microscopic scale. Traditionally used in biological imaging [18, 19], this technique has recently been applied in cultural heritage to create virtual cross-sections of paintings [20], differentiate red organic dyes [21], and identify the vermilion degradation product in a 14th-century painting [22].

In this study, we present pump-probe imaging of artificially aged CdS paints which are prepared according to historical recipes. We demonstrate that pump-probe microscopy can noninvasively monitor the degradation inside single grains during artificial aging with micrometer-scale resolution. In addition, early-stage alterations on CdS mock-up paints can be recognized before visual changes are apparent, highlighting the potential of pump-probe microscopy to detect the degradation of seemingly well-preserved artworks.

2. Methods

2.1. Pump-probe microscopy

The principle of pump-probe microscopy can be found in previous reviews [23, 24] and will only be briefly described here. The experimental setup is shown in figure 1(a). The pump-probe approach generates contrast by nonlinear optical interactions between the sample and two synchronized femtosecond pulse trains of different wavelengths. The two pulse trains, pump and probe, have pulse lengths of ∼150 fs and are generated from an 80 MHz mode-locked Ti: sapphire laser (Chameleon, Coherent) and an optical parametric oscillator (Mira-OPO, Coherent). We operate the microscope at a 720 nm pump and 817 nm probe wavelength combination with 0.4 mW of optical power in each beam. The pump pulse train is amplitude-modulated at 2 MHz by an acousto-optic modulator and superimposed with the probe pulse train before entering the laser scanning microscope. There they are focused on the sample with an objective lens (Olympus UPlanApo 20x objective, NA = 0.7; focal size ∼0.6 μm for both beams) and scanned through the sample areas. Pump and probe pulse trains interact nonlinearly with the sample in the focal region, thereby transferring some amplitude modulation from the pump to the probe pulse train (see figure 1(b)). The backscattered probe light is collected while the pump light is removed with a filter, and the amplitude modulation of the probe pulses is measured with a photodiode and a lock-in amplifier. Changing the inter-pulse time delay (τ) between pump and probe with a motorized translational stage results in characteristic transient absorption curves; changing the beam position (x,y along the lateral direction and z in the axial direction) yields three-dimensional volumetric data.

Many nonlinear interactions are accessible with pump-probe microscopy. For semiconductors, such as CdS, pump-probe can, in principle, probe charge carrier dynamics near the band edge or in trap states (see the supporting figures SI2 and SI3 for more details and [25] for an application of our microscope to

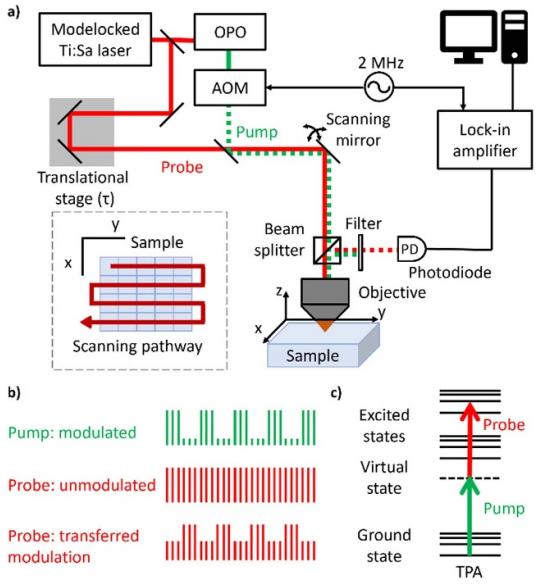

Figure 1. Pump-probe microscopy. (a) Simplified schematic of the experimental setup. For details, see the supporting information. (b) Modulation transfer scheme. (c) Two-photon absorption (TPA). The dashed line indicates a virtual state.

energy-harvesting semiconductors). However, our laser system is currently restricted to pump wavelengths below the band edge. Hence, excitation requires both pump and probe pulses and leaves two-photon absorption (TPA, see figure 1(c)) as the predominant interaction between the pulses and CdS. Because both pump and probe wavelengths are substantially below the band edge, reabsorption effects, which can affect some reflectance measurements, are absent in our pump-probe images. TPA involves a virtual energy state, and the sample absorbs one photon from each pulse only when pump and probe pulses arrive simultaneously at the sample ($\tau = 0$ ps). The multiphoton nature of pump-probe microscopy allows for virtual sectioning and volumetric imaging in heterogeneous paint samples. By scanning the focus of the laser beams across the sample in both lateral directions and moving the sample in the axial direction, we can non-destructively map CdS grains within paints. This allows us to monitor CdS changes during artificial aging by recording the reduction of TPA signals.

2.2. Pigment preparation and analytical methods

Cadmium sulfide oil paints were prepared from both in-house synthesized and commercially available (Sigma Aldrich) pigments. The oil paints were then aged under different relativ humidity levels and light exposure. The aged and control samples were investigated by pump-probe microscopy throughout the aging period and by UV-VIS-NIR, FTIR, and XPS spectroscopy before and after aging. An overview of the synthetic procedures, paint preparation, aging procedures, and analytical methods is given below, for further details we refer to the supporting information.

3. Results and discussion

3.1. Reproduction and characterization of historical CdS pigments

To simulate the degradation in historical paintings through artificial aging, CdS was reproduced following historical wet methods. CdS pigments synthesized from wet methods are more susceptible to degradation because of the poor crystalline structure and potential synthetic residues [5, 14]. $CdCl_2$ was chosen as a starting agent because chloride was found in degraded regions in multiple paintings [5], making it one of the most plausible ingredient of the historical manufacturing process. Na_2S was selected as sulfur source since previous research showed that CdS made from Na_2S had similar morphology and photoluminescence properties as historical pigments [26]. This wet method reaction is described below (detailed synthetic procedures can be found in the supporting information).

$$CdCl_2 + Na_2S \rightarrow CdS + 2NaCl.$$

Commercial CdS was purchased to make reference samples, and both synthesized and commercial CdS powders were first characterized and then prepared as oil paints to be artificially degraded. Figure 2 displays commercially available (top row) and synthesized (bottom row) CdS samples: powders (a), (d), derived

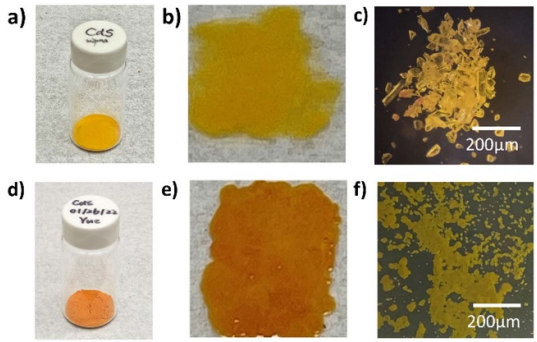

Figure 2. Commercial and synthesized CdS. Commercial CdS (Sigma Aldrich): (a) powder, (b) linseed oil paint, and (c) microscopic image. Synthesized CdS: (d) powder, (e) linseed oil paint, and (f) microscopic image. Commercial CdS contains large, semitransparent crystals, while synthesized CdS displays smaller grains without clear crystalline structures.

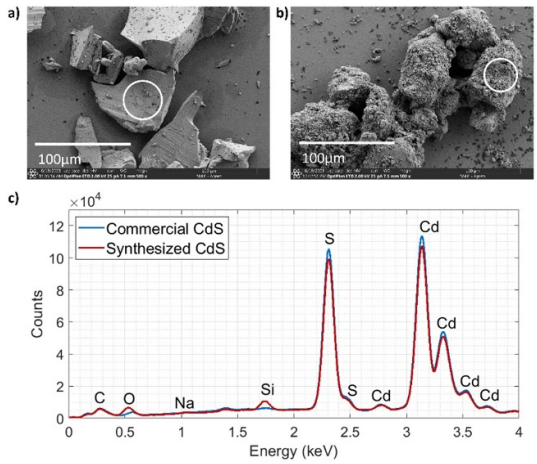

Figure 3. SEM-EDS analysis of commercial and synthesized CdS. SEM images of (a) commercial and (b) synthesized CdS. (c) EDS spectra of commercial (blue) and synthesized (red) CdS. Both show the elemental components in the circled regions of their corresponding SEM images.

linseed oil paints (b), (e), and microscopic images (c), (f). The particle morphology and crystal forms were characterized by SEM-EDS (scanning electron microscopy - energy disperse x-ray spectroscopy) images (figure 3) and x-ray diffraction (XRD) spectra (figure 4).

The SEM image of figure 3(a) indicates that commercial CdS has a smooth surface with a well-defined crystalline structure in agreement with the microscopic photos. The EDS spectrum of commercial CdS in figure 3(c) shows a high purity of CdS with a minor amount of C (which may originate from sample processing). The synthesized CdS is composed of grains with a rough surface and nanometer-sized particles, as shown in figure 3(b). The corresponding EDS spectrum shows small contributions from C, O, Si (possibly comes from the imaging substrate), and negligible amount of Na (synthetic residue) in addition to the expected Cd and S. There was no detectable amount of Cl, which suggests an effective washing process in synthesis procedures. The magnified SEM image (shown in figure SI4) reveals the existence of aggregated grains from nano-scale particles. The nano-dimensional and aggregated particles have a larger surface-to-volume ratio than commercial CdS grains, which could reduce the specular reflectance and lead to a darker color than commercial CdS.

Figure 4(a) shows XRD spectra of the two CdS powders with reference lines [27, 28] for hexagonal and cubic CdS. The declining baseline for low scattering angles is caused by the linseed oil binder (see figure SI6(b) in the supporting information). The commercial CdS shows a clear hexagonal structure, while the synthesized CdS exhibits a more cubic and amorphous structure. The crystal structure difference can also contribute to the color difference of two CdS (where commercial CdS shows a lighter color) [29]. In addition, the broad XRD peaks of synthesized CdS are a sign of imperfect crystal lattice and nanometric crystal size [30]. UV-VIS-NIR reflectance spectra shown in figure SI5(a) also confirm the color difference between two CdS samples. The sigmoidal-shaped reflectance spectrum of synthesized CdS is another sign of poor crystal structure [5, 31]. The fluorescence spectra (shown in figure SI5(b)) show that commercial CdS

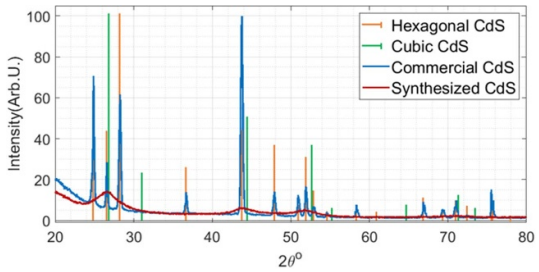

Figure 4. XRD spectra of CdS and references (hexagonal and cubic) crystal structures. Commercial CdS shows strong hexagonal peaks, while synthesized CdS shows a cubic and amorphous structure.

Table 1. Photographs of synthesized CdS oil paints before and after aging[a].

Aging conditions	Unaged sample	Aged for one week	Aged for two weeks	Aged for four weeks
Light + high RH level				
Dark + high RH level				

[a] $Sample_{BL}$ and $Sample_{N/A}$ are not shown here since they did not show visible signs of degradation over four weeks. This is consistent with pump-probe experiments discussed later.

has a sharp band gap emission at 512 nm which is typical for bulk CdS. The synthesized CdS presents no band gap emission, similar to archived historical CdS pigments examined in a previous study [2].

3.2. Artificial aging of CdS paints

Artificial aging of both CdS paints was performed in a homemade aging chamber [12]. The CdS paints were applied on microscope slides and aged by blue light (BL) irradiation at a wavelength of ∼400 nm and exposure to high relative humidity (RH) levels (∼75%) for four weeks. These samples were labeled as $Sample_{BL+RH}$. Control experiments were also performed in which identical samples were exposed to only light ($Sample_{BL}$) or only high RH levels ($Sample_{RH}$) or left in a dark and dry environment ($Sample_{N/A}$). Pump-probe microscopy was utilized to monitor the change in CdS paints during the four weeks of aging. The commercial CdS samples exposed to both light and high RH levels ($Sample^{com}$) showed only negligible signs of degradation; therefore, we focus on the synthesized CdS sample for the following sections, unless otherwise noted. More details on sample preparation, aging chamber design, and aging process are documented in the supporting information.

Table 1 presents photos of synthesized CdS paints before and after aging with light and high RH levels. The paints did not exhibit apparent signs of degradation during the first two weeks, but slight alterations, such as a global loss of surface oil gloss, became visible after four weeks. The samples exposed to only high RH levels retained their oil gloss, suggesting a lower degree of degradation in comparison to the light-exposed sample.

The $Sample_{BL+RH}$ exhibited a slight color change apparent to the eye. As confirmation, we acquired a UV-VIS-NIR reflectance spectrum of this sample and an unaged reference sample, shown in figure 5. In agreement with visual observations, the reflectance curve of $Sample_{BL+RH}$ exhibited a blue shift indicating a color change of the paint to lighter shades of yellow. The reflectance spectra of pure linseed oil are shown in the supporting information (figure SI6(a)).

3.3. Pump-probe signatures of CdS paints and visualization of CdS degradation

To monitor the degradation progress on a microscopic scale, pump-probe microscopy was used to image CdS paints after various durations of artificial aging. Two sets of samples were degraded for each aging condition, and two regions of interest (ROIs) in the central area of each sample were investigated. We observed a qualitatively similar degree of degradation in each ROI. Pump-probe images of the same ROI on $Sample_{BL+RH}$ before, after two weeks, and after four weeks of aging are shown in figures 6(a)–(c). CdS grains are dominated by an instantaneous TPA signal, which can be seen in the transient absorption curves averaged over the rectangular areas plotted in figure 6(d). The signal decreases by 20%–30% during the first two weeks of aging and by more than 80% during weeks two to four.

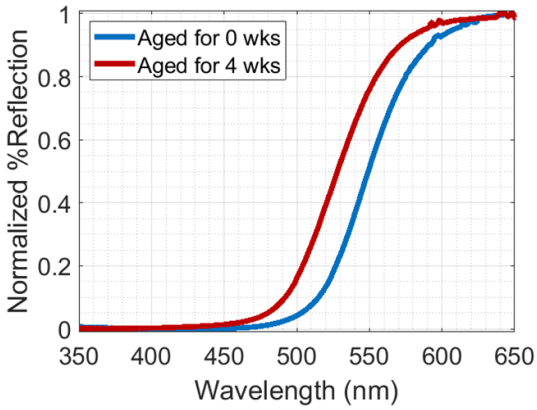

Figure 5. UV-Vis-NIR reflectance spectra of $\text{Sample}_{\text{BL+RH}}$ before and after aging.

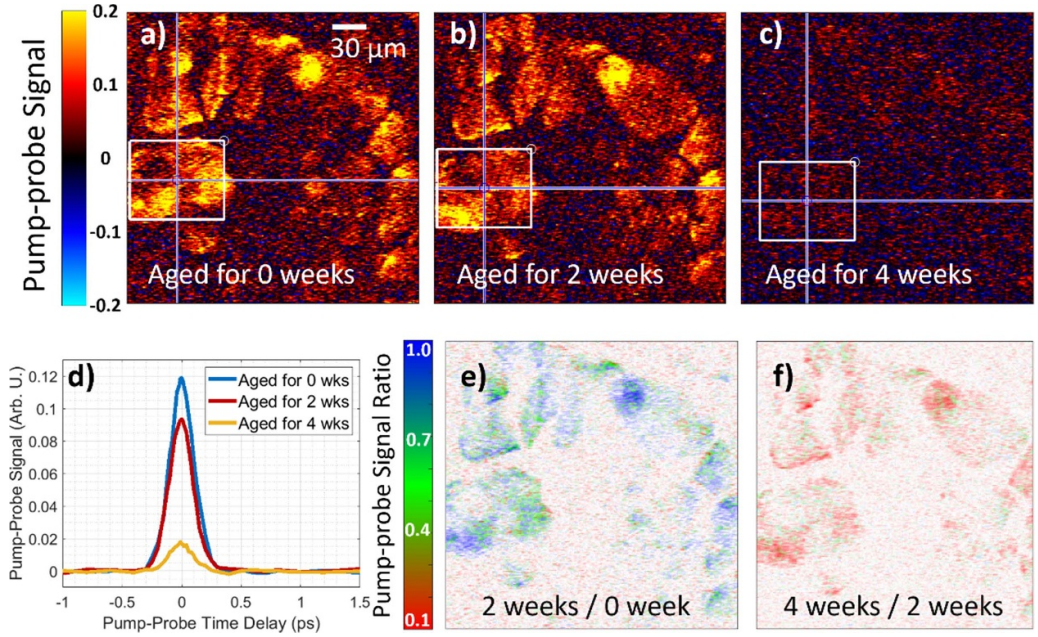

Figure 6. Pump-probe false-color images of $\text{Sample}_{\text{BL+RH}}$ (a) before aging, (b) aged for two weeks, and (c) aged for four weeks. (d) Pump-probe transient absorption curves spatially averaged over the white rectangle in the pump-probe images. Pump-probe pixel-by-pixel ratio images of (e) two weeks over zero weeks of aging and (f) four weeks over two weeks of aging.

To map the change in pump-probe signals of CdS during aging, we co-registered pump-probe images of aged and unaged paints and computed the ratio of TPA signal between aged and unaged CdS. Figure 6(e) shows a pixel-by-pixel ratio image between two weeks of aging and no aging (figure 6(b) divided by figure 6(a)). This ratio image represents the signal loss over two weeks of artificial aging. The false coloring is chosen such that unaltered regions are displayed in blue, and areas with drastically diminished signals are displayed in red. Green shows a moderate level of degradation. Similarly, figure 6(f) shows the ratio image between four weeks of aging and two weeks of aging (figure 6(c) divided by figure 6(b)). Beyond four weeks of aging, the pump-probe signal decreased to unobservable levels, limited by the signal-to-noise performance of our microscope. The pump-probe signatures of degradation are more severe in the second two weeks of aging (weeks two to four). Changes after two weeks were not yet observable by visual inspection or by bright field microscopy, but were obvious in the pump-probe data, emphasizing the ability of pump-probe to detect early-stage degradation.

To visualize early-stage degradation in three dimensions on the surface and the interior of the paint, $\text{Sample}_{\text{BL+RH}}$ was investigated after aging for one week (no degradation visible in color or gloss, neither by eye nor by bright field microscopy). We were able to image through the entire paint layer (typically 30 μm thick) in steps of 1 μm. Figure 7 shows a volume ratio image between one week of aging and no aging. A video of a full three-dimensional scan through this volume can be found in the Supporting Information.

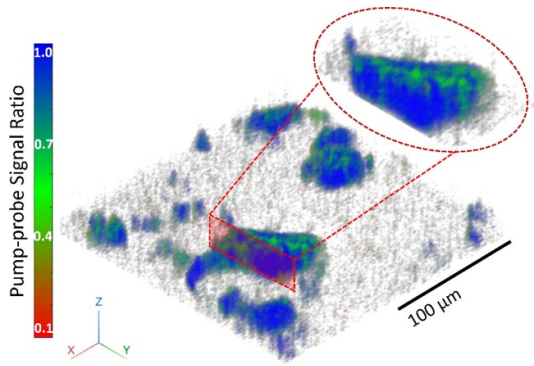

Figure 7. Three-dimensional ratio image of $Sample_{BL+RH}$ aged for one week. The small grains and the surface of large grains experienced moderate levels of degradation, while the inside of large grains showed no signs of degradation. The insert shows a cross-section of a large CdS grain that displays no degradation (blue) inside with moderate degradation (green) on the surface. Volume dimension is (230 × 230 × 30) μm.

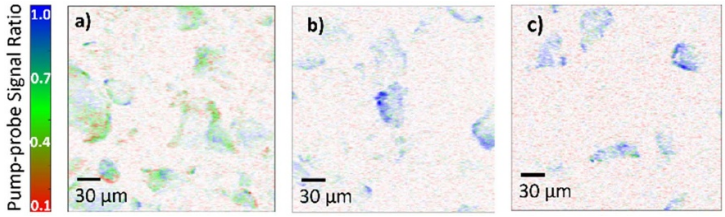

Figure 8. Pump-probe ratio images of four weeks over zero weeks of aging. (a) Only exposed to moisture ($Sample_{RH}$). (b) Only exposed to light ($Sample_{BL}$). (c) No exposure (kept in the dark and low RH levels, sample $_{N/A}$).

Small (less than a few μm) grains exhibited a moderate degree of CdS degradation (green color) throughout the entire grains. Large grains showed degradation that was localized only to the top surface (~5 μm–10 μm depth). The inside of the large grains remained unaffected (blue color). These observations indicate a particle size influence on the degradation of CdS: smaller particles experience more degradation in a shorter period of time. This result supports the previous hypothesis that CdS paints containing nano-sized particles experience more intense degradation [10].

To understand the individual effects of moisture and light on the degradation of synthesized CdS pigments, figure 8 shows the loss of signals in the control samples after four weeks of aging. $Sample_{RH}$ exhibited moderate degradation with 30%–60% pump-probe signal decline (figure 8(a)), which is less compared with the about 85% signal decrease (25% in weeks 0-2 and 80% in weeks 2-4) of $Sample_{BL+RH}$. This result further supports previous findings that the moisture mainly triggers the degradation of CdS paints [5, 12]. $Sample_{BL}$ showed only minor signs of degradation after four weeks (figure 8(b)), indicating that light itself is not a sufficient factor to degrade CdS within the duration of exposure. $Sample_{N/A}$ showed no sign of pump-probe signal decrease within four weeks (figure 8(c)), indicating that the pump-probe signal change did not result from factors other than light and moisture.

The commercial CdS paint ($Sample^{com}$) showed no detectable pump-probe signal decrease even after eight weeks of aging by both light and high RH levels (see figure 9), demonstrating the stability of modern CdS samples with well-defined crystal structure and negligible amounts of defects.

3.4. FTIR and XPS techniques confirmed the degradation of CdS paints

FTIR spectroscopy is usually regarded as a nondestructive technique. However, the attenuated total reflectance (ATR) mode requires physical contact between the sample and detection crystal, which would have distorted the paint layer (rearranged individual pigments in our paint samples) and altered the surfaces. Therefore, FTIR-ATR experiments were only performed after the four-week aging period and after pump-probe imaging. The common degradation products and impurities found in historical CdS paintings, including $CdSO_4$, $CdCO_3$, and $CdCl_2$ [4, 5, 11], were also studied individually to serve as reference chemicals and to compare with aged paints. The product details, data processing procedures, and FTIR spectra (figure SI7) of reference chemicals can be found in the Supporting Information.

The FTIR spectra of $Sample_{N/A}$ feature notable CH stretching (at 2853 and 2924 cm^{-1}) and CO stretching peaks (1737 cm^{-1}). These peaks are typical fingerprints of linseed oil binder used to prepare paint

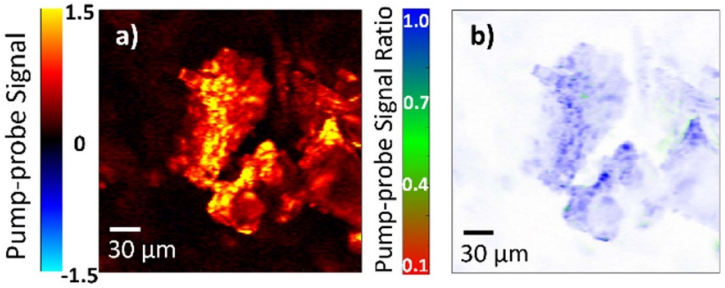

Figure 9. False-color (a) pump-probe image and (b) pixel-by-pixel ratio image (aged for eight weeks/before aging) of commercial CdS (Sample^{com}).

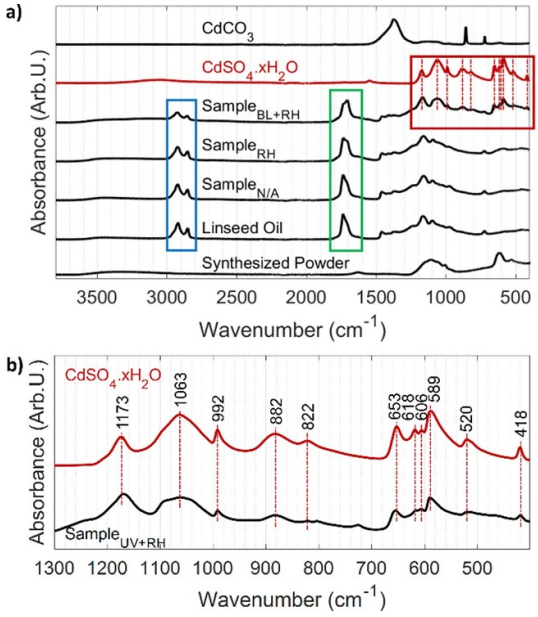

Figure 10. FTIR spectra of synthesized CdS powder, linseed oil binder, unaged and aged synthesized CdS paints, $CdSO_4{\cdot}xH_2O$ (Sigma Aldrich), and $CdCO_3$ (Sigma Aldrich). (a) Blue rectangle: CH stretching peaks at 2853 cm^{-1} and 2924 cm^{-1} decreased after aging, indicating the degradation of linseed oil binder; Green rectangle: decrease of CO stretching peak (1737 cm^{-1}) and increase of free fatty acids peaks (1708–1713 cm^{-1}); Red rectangle: aged CdS paint shows pronounced overlap with $CdSO_4{\cdot}xH_2O$ (details in 10b). (b) $Sample_{BL+RH}$ shows pronounced correspondence with $CdSO_4{\cdot}xH_2O$, indicating the degradation products of the paint.

samples. For $Sample_{RH}$, the oil peaks moderately declined and a new peak of free fatty acids at 1708–1713 cm^{-1} appeared, revealing the breakdown of the binder; no other changes were observed from the FTIR spectra of this sample. $Sample_{BL+RH}$ displayed a more distinguished decrease of linseed oil peaks and an increase of free fatty acids, representing a higher degree of oil degradation. In addition, new spectral peaks appeared at 1173,1063, 992, 882, 822, 653, 618, 606, 589, 520 and 481 cm^{-1} (see figure 10(b)), which match the commercial $CdSO_4{\cdot}xH_2O$ reference. Therefore, we conclude that the CdS was converted into $CdSO_4{\cdot}xH_2O$ under light exposure and high RH levels. No other reference chemicals or degradation products from the literature [12] were identified in degraded paints. FTIR analysis unambiguously confirms that we successfully degraded CdS. These spectra also demonstrate that the transition from CdS to $CdSO_4$ happens predominantly under exposure to both light and high RH levels.

In addition, commercial CdS paint (Sample^{com}) exhibits no sign of degradation other than the increase of free fatty acid peaks (figure SI8). This further supports the pump-probe findings that commercial CdS did not degrade during aging.

XPS experiments were carried out on synthesized CdS pigment powders and $Sample_{BL+RH}$ to compare the chemical state of sulfur components. The paint sample before aging was not investigated in this experiment since x-rays get absorbed in the oil-rich surface of newly prepared paints. The S 2p spectra can reflect the amount of each sulfur species in the two samples, thus indicating the evolution of sulfur components. The spectra show 87% of S^{2-} and 13% of SO_4^{2-} in synthesized CdS powders (figure 11(a)). After artificial aging, the S^{2-} on the sample surface decreased to 33%, and the SO_4^{2-} increased to 67%

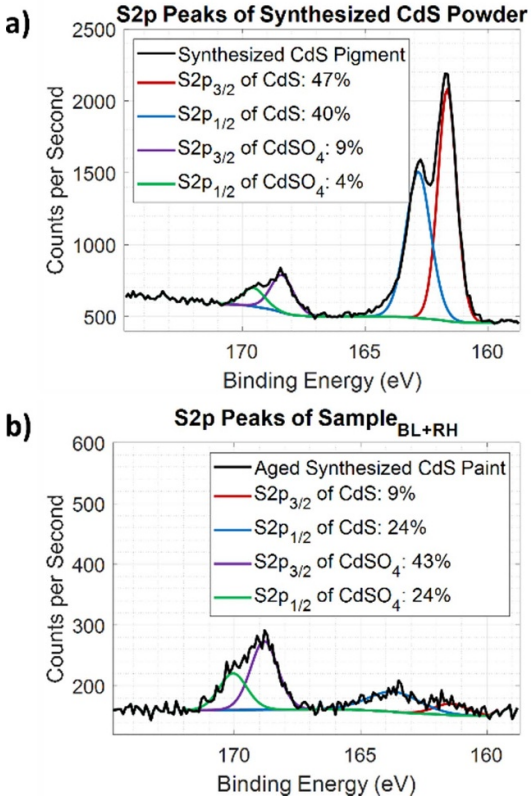

Figure 11. XPS S 2p spectra of (a) synthesized CdS powders and (b) $Sample_{BL+RH}$. The red, blue, purple, and green curves are fitted data of S 2p peaks of CdS and $CdSO_4$ components. The molar/area percentage values are labeled for each component. The composition of $CdSO_4$ increased from 13% to 67% after artificial aging.

(figure 11(b)), emphasizing the oxidation of sulfur from S^{2-} to SO_4^{2-} during aging. Again, the XPS spectra verified the conclusions drawn from pump-probe microscopy and FTIR experiments, that the CdS turned into $CdSO_4$ during aging by light and high RH levels. This conclusion is also consistent with the findings in previous research [12].

4. Conclusion

We demonstrated the use of pump-probe microscopy to visualize CdS degradation in cadmium yellow paints, in particular the onset of degradation before visible changes can be observed. CdS was produced following historical synthesis methods and exhibits distinctive properties: poor crystalline structures, aggregated grains with nano-dimensional particles, and no band gap emission. These properties are similar to those of archived historical pigments making these samples ideal candidates for artificial aging experiments. Mock-up paints prepared from synthesized CdS were artificially aged to generate degradation similar to those found in historical artworks. We showed that pump-probe microscopy can nondestructively create 3-dimensional visualizations of CdS degradation in paints on the microscopic scale. In summary, we draw the following conclusions:

1. Pump-probe microscopy can detect the onset of CdS degradation through a decline of the TPA signal. This signal decrease is already observable after a few weeks of aging, suggesting that degradation happens microscopically before macroscopic observations are possible.
2. In-situ, nondestructive pump-probe imaging can track degradation of paint samples during the aging process. Three-dimensional pump-probe images show that degradation starts primarily in smaller grains and on the surface of large grains.
3. The stability of CdS paints is affected by the degree of crystallinity of pigments and aging conditions. Commercial CdS with well-defined crystal structures displayed no change in pump-probe signal, even after eight weeks of aging, while synthesized CdS with poor crystal structures showed obvious changes in pump-probe signatures within one to two weeks. For synthesized CdS paints, humidity is necessary to induce degradation, while light is an accelerator to turn CdS into $CdSO_4 \cdot xH_2O$.

Overall, pump-probe microscopy can provide in-situ, early-stage detection of CdS degradation on the micrometer scale. We believe that pump-probe microscopy is a valuable technique to nondestructively investigate pigment degradation, for example to study the role of leftover synthetic residues or secondary products (such as $CdCl_2$ and $CdSO_4$) in the degradation process of CdS paints. Future investigations can be carried out on the microscopic degradation behaviors of paint samples with impurities or mixed with other historical pigments.

Data availability statement

The data cannot be made publicly available upon publication because no suitable repository exists for hosting data in this field of study. The data that support the findings of this study are available upon reasonable request from the authors.

Acknowledgments

This material is based upon work supported by the National Science Foundation, Division of Chemistry under Award No. CHE-2108623 (M C F). Martin Fischer also received salary support from the Chan Zuckerberg Initiative (Grant No. 2021-242921). We would like to thank Dr John Delaney, Dr Mathieu Thoury, Dr Daniela Comelli, and Dr Marta Ghirardello for their valuable assistance and discussions. We also thank Heidi Kastenholz and Dr Jake Lindale for helpful discussions.

The SEM-EDS, XRD, and XPS experiments were performed at the Duke University Shared Materials Instrumentation Facility (SMIF), a member of the North Carolina Research Triangle Nanotechnology Network (RTNN), which is supported by the National Science Foundation (Award Number ECCS-2025064) as part of the National Nanotechnology Coordinated Infrastructure (NNCI). The photoluminescence experiments were performed in the Duke Advanced Light Imaging and Spectroscopy Facility (ALIS).

ORCID iDs

Yue Zhou https://orcid.org/0009-0005-9397-0915
David Grass https://orcid.org/0000-0003-1781-0969
Warren S Warren https://orcid.org/0000-0001-8458-2076
Martin C Fischer https://orcid.org/0000-0002-3397-4181

References

[1] Fiedler I and Bayard M 1986 Cadmium yellows, oranges and reds *Artists' Pigments: A Handbook of Their History and Characteristics* ed R L Feller (National Gallery of Art) pp 65–108
[2] Ghirardello M, Mosca S, Marti-Rujas J, Nardo L, Burnstock A, Nevin A, Bondani M, Toniolo L, Valentini G and Comelli D 2018 Time-resolved photoluminescence microscopy combined with x-ray analyses and raman spectroscopy sheds light on the imperfect synthesis of historical cadmium pigments *Anal. Chem.* **90** 10771–9
[3] Roy A 2007 Monet's palette in the twentieth century: water-lilies and irises *National Gallery Technical Bulletin* vol 28 (National Gallery Company Limited) pp 58–68 (available at: www.jstor.org/stable/i40097093)
[4] Van der Snickt G, Janssens K, Dik J, De Nolf W, Vanmeert F, Jaroszewicz J, Cotte M, Falkenberg G and Van der Loeff L 2012 Combined use of synchrotron radiation based micro-x-ray fluorescence, micro-x-ray diffraction, micro-x-ray absorption near-edge, and micro-fourier transform infrared spectroscopies for revealing an alternative degradation pathway of the pigment cadmium yellow in a painting by Van Gogh *Anal. Chem.* **84** 10221–8
[5] Monico L *et al* 2020 Probing the chemistry of CdS paints in the scream by in situ noninvasive spectroscopies and synchrotron radiation x-ray techniques *Sci. Adv.* **6** eaay3514
[6] Mass J, Sedlmair J, Patterson C S, Carson D, Buckley B and Hirschmugl C 2013 SR-FTIR imaging of the altered cadmium sulfide yellow paints in Henri Matisse's Le Bonheur de vivre (1905–6)–examination of visually distinct degradation regions *Analyst* **138** 6032–43
[7] Mass J L, Opila R, Buckley B, Cotte M, Church J and Mehta A 2013 The photodegradation of cadmium yellow paints in Henri Matisse's Le Bonheur de vivre (1905–1906) *Appl. Phys.* A **111** 59–68
[8] Pouyet E *et al* 2015 2D x-ray and FTIR micro-analysis of the degradation of cadmium yellow pigment in paintings of Henri Matisse *Appl. Phys.* A **121** 967–80
[9] Voras Z E, deGhetaldi K, Wiggins M B, Buckley B, Baade B, Mass J L and Beebe T P 2015 ToF–SIMS imaging of molecular-level alteration mechanisms in Le Bonheur de vivre by Henri Matisse *Appl. Phys.* A **121** 1015–30
[10] Comelli D, MacLennan D, Ghirardello M, Phenix A, Schmidt Patterson C, Khanjian H, Gross M, Valentini G, Trentelman K and Nevin A 2019 Degradation of cadmium yellow paint: new evidence from photoluminescence studies of trap states in Picasso's Femme (Époque des "Demoiselles d'Avignon") *Anal. Chem.* **91** 3421–8
[11] Van der Snickt G, Dik J, Cotte M, Janssens K, Jaroszewicz J, De Nolf W, Groenewegen J and Van der Loeff L 2009 Characterization of a degraded cadmium yellow (CdS) pigment in an oil painting by means of synchrotron radiation based x-ray techniques *Anal. Chem.* **81** 2600–10
[12] Monico L, Chieli A, De Meyer S, Cotte M, de Nolf W, Falkenberg G, Janssens K, Romani A and Miliani C 2018 Role of the relative humidity and the Cd/Zn stoichiometry in the photooxidation process of cadmium yellows ($CdS/Cd_{1-x}Zn_xS$) in oil paintings *Chem. Eur. J.* **24** 11584–93

[13] Thoury M, Delaney J K, de la Rie E R, Palmer M, Morales K and Krueger J 2011 Near-infrared luminescence of cadmium pigments: in situ identification and mapping in paintings *Appl. Spectrosc.* **65** 939–51
[14] Church A H 1915 *The Chemistry of Paints and Painting* (Seeley, Service & Co. Limited)
[15] Laurie A P 1895 *Facts about Processes, Pigments and Vehicles: A Manual for Art Student* (Macmillan and Co)
[16] Cesaratto A, Leona M, Lombardi J R, Comelli D, Nevin A and Londero P 2014 Detection of organic colorants in historical painting layers using UV laser ablation surface-enhanced raman microspectroscopy *Angew. Chem., Int. Ed.* **53** 14373–7
[17] Miliani C, Monico L, Melo M J, Fantacci S, Angelin E M, Romani A and Janssens K 2018 Photochemistry of artists' dyes and pigments: towards better understanding and prevention of colour change in works of art *Angew. Chem., Int. Ed.* **57** 7324–34
[18] Grass D, Beasley G M, Fischer M C, Selim M A, Zhou Y and Warren W S 2022 Contrast mechanisms in pump-probe microscopy of melanin *Opt. Express* **30** 31852–62
[19] Kuk-Youn J, Simone D, Martin C F, Kevin C Z, Xiaomeng J, Jin Y and Warren S W 2019 Unraveling the molecular nature of melanin changes in metastatic cancer *J. Biomed. Opt.* **24** 051414
[20] Villafana T E, Brown W P, Delaney J K, Palmer M, Warren W S and Fischer M C 2014 Femtosecond pump-probe microscopy generates virtual cross-sections in historic artwork *Proc. Natl Acad. Sci.* **111** 1708–13
[21] Yu J, Warren W S and Fischer M C 2018 spectroscopic differentiation and microscopic imaging of red organic pigments using optical pump–probe contrast *Anal. Chem.* **90** 12686–91
[22] Yu J, Warren W S and Fischer M C 2019 Visualization of vermilion degradation using pump-probe microscopy *Sci. Adv.* **5** eaaw3136
[23] Fischer M C, Wilson J W, Robles F E and Warren W S 2016 Invited review article: pump-probe microscopy *Rev. Sci. Instrum.* **87** 031101
[24] Melo M J *et al* Laboratory instrumentation (Springer) pp 1–36
[25] Yu J, Li Z, Liao Y, Kolodziej C, Kuyuldar S, Warren W S, Burda C and Fischer M C 2019 Probing the spatial heterogeneity of carrier relaxation dynamics in $CH_3NH_3PbI_3$ perovskite thin films with femtosecond time—resolved nonlinear optical microscopy *Adv. Opt. Mater.* **7** 1901185
[26] Ghirardello M 2021 Study of the physical-chemical properties of cadmium yellow: understanding how synthesis methods impact on paint stability, physics department (The Polytechnic University of Milan) p 161
[27] Sowa H 2005 On the mechanism of the pressure-induced wurtzite- to NaCl-type phase transition in CdS: an x-ray diffraction study *Solid State Sci.* **7** 73–78
[28] Noor N A, Ikram N, Ali S, Nazir S, Alay-e-abbas S M and Shaukat A 2010 First-principles calculations of structural, electronic and optical properties of $Cd_xZn_{1-x}S$ alloys *J. Alloys Compd.* **507** 356–63
[29] Ghirardello M, Otero V, Comelli D, Toniolo L, Dellasega D, Nessi L, Cantoni M, Valentini G, Nevin A and Melo M J 2021 An investigation into the synthesis of cadmium sulfide pigments for a better understanding of their reactivity in artworks *Dyes Pigments* **186** 108998
[30] Raja P B, Munusamy K R, Perumal V and Ibrahim M N M 2022 5—Characterization of nanomaterial used in nanobioremediation *Nano-Bioremediation: Fundamentals and Applications* ed H M N Iqbal, M Bilal and T A Nguyen (Elsevier) pp 57–83
[31] Deng H and Hossenlopp J M 2005 Combined x-ray diffraction and diffuse reflectance analysis of nanocrystalline mixed Sn(II) and Sn(IV) oxide powders *J. Phys. Chem.* A **109** 66–73